Analysis and Comparison of Multi-Coil Inductive Power Transfer Systems

Venugopal Prasanth, Soumya Bandyopadhyay, Pavol Bauer and Jan Abraham Ferreira
Dept. Electrical Sustainable Energy, DCE&S group
TU Delft, Mekelweg 04, 2628 CD, Delft, the Netherlands
Email: v.prasanth@tudelft.nl, s.bandyopadhyay@tudelft.nl, p.bauer@tudelft.nl and j.a.ferreira@tudelft.nl

***Abstract*—This paper presents a comparative analysis of Multi-Coil Inductive Power Transfer (MCIPT) systems. A multi-coil magnetic system can be decomposed into a single system of coils using matrix manipulation when the system is linear. A comparitive analytical study of air-cored coils to estimate the magnetic parameters - L, M, k of several coil shapes - circular, rectangular, square, segmented circular and segmented rectangular (DD) is then carried out. A misalignment shape characteristic is obtained and comparisons brought out. Important criteria to be considered for misalignment tolerant MCIPT is also described. A boundary for performance limits of misaligned multi-coil IPT systems is presented.**

I. Introduction

Wireless Inductive Power Transfer (IPT) is a technique for electromagnetic energy transfer using loosely coupled coils to remove wired interconnects. The principle of operation involves the nullification of reactive power demands of the primary/transmitter and secondary/pickup by carefully designing compensating capacitors to both the coils. Then, the system operates in a double resonant mode with both primary and secondary at resonance, enhancing the power transferred, power factor brought to unity and improving system efficiency [1].

The non-contact nature makes it possible to transfer power without fear of shock or sparks. Apart from removing messy cord, they also dont leave behind any residue and also need reduced maintenance. Hence, they can be used in all extreme environmental conditions viz. clean-room systems, dirty mining operations and even for underwater power delivery [2]. A number of applications from health care to EVs ranging in all power scales (mW to MW) are being developed using the principles of IPT [2], [3], [4].

A major limitation that IPT system magnetics has is the tolerance to misalignment. Misalignment tolerant IPT systems is a major requirement for charge pads in both movable electronics and e-mobility applications. For such a tolerant design, multi-coil IPT systems are being developed. A decoupled rectangular (DD) charge pad is presented in [5]. Also, DD coils which are displaced over each other, is referred to as bipolar pad. Here, unintended power flow due to the mutual inductance between the coils in a primary (also in secondary) is made zero [5].

In this paper, we establish a theoretical framework to evaluate the magnetic parameters of MCIPT in general. A description of fundamentals is presented in Section II. Based on linearity, a $'n'$-coupled primary system with a $'m-n'$ coupled secondary ($L_{(m\times m)}$ magnetic system) can be reduced to a single-primary single-secondary system ($L_{(2\times 2)}$ magnetic system). This theoretical framework is derived in Section III. A number of design considerations including the shape dependent misalignment characteristic is presented in Section IV. The performance parameters and their influence on the magnetic design is focused specifically in Section V. Performance limitations of IPT system under misalignment conditions is dealt with in Section VI. Finally, Section VII presents the conclusions.

II. IPT System Fundamentals

A loosely coupled IPT transformer consists of two charge pads with inductances L_1, L_2 that are separated from each other with a large air gap. If M is the mutual inductance between the two, the maximum apparent power that can be transferred to the secondary, S_{max} is related to the maximum voltage that can be induced in the secondary, V_{oc} and the maximum current that the secondary can source, I_{sc} as

$$S_{max} = V_{oc} \times I_{sc} \tag{1}$$

If I_1 is the primary current of the IPT transformer sourced at frequency ω , $V_{oc} = j\omega M I_1$ and $I_{sc} = \dfrac{V_{oc}}{j\omega L_2} = \dfrac{M I_1}{L_2}$. This factor, S_{max} is also called the uncompensated reactive power of the pickup. Now, on connecting capacitors to both the primary and secondary and them being designed suitably, double resonance takes place, both at the primary as well as the secondary. As a result, either the current (Series Resonance) or the voltage (Parallel Resonance) is amplified by the Q factor of the respective circuit. Power transferred to the secondary, P_2 is related to the quality factor of the secondary circuit $Q_{(2,L)}$ (loaded quality factor) as

$$P_2 = \frac{(I_1^2 M^2 Q_{(2,L)} \omega)}{L_2} \tag{2}$$

It is useful to also consider that literature often reports two quality factors, they are called the native/unloaded and loaded quality factors respectively and their difference need to be distinguished [6]. The native quality factor is used to quantify the ratio of a coil's inductive reactance to its resistance $Q = (\omega \times L)/R_{coil})$, while the loaded quality factor is defined in terms of the load resistance, R_L as $Q_L = (\omega \times L)/(R_L + R_{coil})$.

The power loss in the IPT system as a rule of thumb is proportional to $\frac{Q}{Q_L}$. Also, considering a constant I and ω_0, the magnetic designer must focus on the ratio (M^2/L_2). This ensures a smaller sized pad, with high efficiency. These are geometry parameters, depending on the size, shape and material of the pads. In addition, M depends on the z-gap between the pads.

III. Multi-Coil Coupled Magnetic Systems

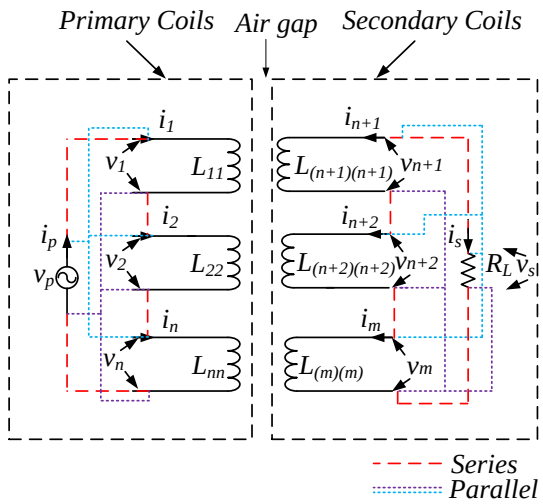

Fig. 1. Defining a IPT system with primary and secondary composed of multiple coils with self-inductances as $(L_{ij}, i = j)$ and mutual inductances as $(L_{ij}, i \neq j)$.

Consider a linear magnetic system consisting of a primary and secondary which are composed of individual coils as shown in 1. The individual coils can be composed in series or parallel to make the primary and secondary respectively. Consider that the primary is composed of $'n'$ coils, $(1,2,..n)$ and the secondary is composed of $'m-n'$ coils, $(n+1,n+2,..m,$ $(m>n))$. In case of such a system, the voltage equation matrix, $[V]$ for all the coils can be written as a function of their currents, $[i]$ and time rate of change of their currents, $\left[\frac{di}{dt}\right]$

$$[V] = [L] \times \left[\frac{di}{dt}\right] + [R] \times [i] \tag{3}$$

Where the matrices are defined as

$$[V] = \begin{bmatrix} v_1 \\ v_2 \\ \vdots \\ v_n \\ v_{n+1} \\ v_{n+2} \\ \vdots \\ v_m \end{bmatrix} \left[\frac{di}{dt}\right] = [i'] = \begin{bmatrix} i'_1 \\ i'_2 \\ \vdots \\ i'_n \\ i'_{n+1} \\ i'_{n+2} \\ \vdots \\ i'_m \end{bmatrix} [i] = \begin{bmatrix} i_1 \\ i_2 \\ \vdots \\ i_n \\ i_{n+1} \\ i_{n+2} \\ \vdots \\ i_m \end{bmatrix} \tag{4}$$

Also, $[R]$ can be defined in terms of the identity matrix I_n as

$$[R] = \begin{bmatrix} R_1 & 0 & 0 & 0 & 0 & 0 & 0 & 0 \\ 0 & R_2 & 0 & 0 & 0 & 0 & 0 & 0 \\ \vdots & \vdots & \vdots & \vdots & \vdots & \vdots & \vdots & \vdots \\ 0 & 0 & 0 & 0 & 0 & 0 & 0 & R_8 \end{bmatrix} \tag{5}$$

Finally, $[L]$ is defined as

$$[L] = \begin{bmatrix} L_{11} & L_{12} & \dots & L_{1n} & L_{1(n+1)} & L_{1(n+2)} & \dots & L_{1(m)} \\ L_{21} & L_{22} & \dots & L_{2n} & L_{2(n+1)} & L_{2(n+2)} & \dots & L_{2(m)} \\ \vdots & \vdots & \vdots & \vdots & \vdots & \vdots & \vdots & \vdots \\ L_{n1} & L_{n2} & \dots & L_{nn} & L_{n(n+1)} & L_{n(n+2)} & \dots & L_{n(m)} \\ L_{(n+1)1} & L_{(n+1)2} & \dots & L_{(n+1)n} & 0 & 0 & 0 & 0 \\ L_{(n+2)1} & L_{(n+2)2} & \dots & L_{(n+2)n} & 0 & 0 & 0 & 0 \\ \vdots & \vdots & \vdots & \vdots & 0 & 0 & 0 & 0 \\ L_{m1} & L_{m2} & \dots & L_{mn} & 0 & 0 & 0 & 0 \end{bmatrix} \tag{6}$$

The series and parallel combination can now be decomposed from this multi-coil combination. In case of a series connected set of coils, $i_p = i_1 = i_2 \cdots = i_n$ and $i_s = i_{n+1} = i_{n+2} \cdots = i_m$. Also, in case of the parallel set of coils, $i_p = i_1 + i_2 \cdots + i_n$ and $i_s = i_{n+1} + i_{n+2} \cdots + i_m$. After such a transformation, it becomes easy to reduce such a system of parallel or series coils into a single coil-pair. In such a system, for both series and parallel system of coils, it can be easy to prove that

$$\begin{bmatrix} \sum_{i=1}^{n} v_i \\ \sum_{j=n+1}^{m} v_j \end{bmatrix} = \begin{bmatrix} \sum_{i=1}^{n}\sum_{j=1}^{n} L_{ij} & \sum_{i=1}^{n}\sum_{j=n+1}^{m} L_{ij} \\ \sum_{j=n+1}^{m}\sum_{i=1}^{n} L_{ij} & \sum_{j=n+1}^{m}\sum_{i=n+1}^{m} L_{ij} \end{bmatrix} \times \begin{bmatrix} i_p{}' \\ i_s{}' \end{bmatrix} + \begin{bmatrix} \sum_{i=1}^{n} R_i & 0 \\ 0 & \sum_{j=n+1}^{m} R_j \end{bmatrix} \times \begin{bmatrix} i_p \\ i_s \end{bmatrix} \tag{7}$$

The eqn. (7) indicates that it is possible to convert a linear

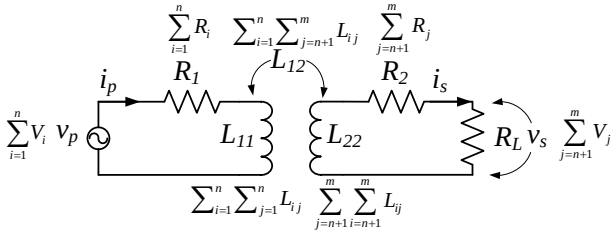

Fig. 2. Equivalent single coil pair for a system of coils with $(1,2..n)$ coils in the primary and $(n+1,n+2..m)$ coils in the pickup.

magnetic system with multi-coil into a system of a single

coil pair by calculating the individual contributions. Such a equivalent coil system is shown in Fig. 2. Such a transposition makes it easy to analytically model multi-coil linear magnetic systems by using the principles of single coils already developed previously.

IV. Design of IPT Coils

A number of steps together can make up a good magnetic design of an IPT charge pad. Depending on the application, it is possible that different shapes can have influence on IPT performance parameters. For multi-coil air-cored IPT systems, it is possible to perform a preliminary analytical study. Such an analysis can be further used to perform numerical studies using FEM analysis for designs considering materials such as ferrites for field shaping and Al for shielding.

A. Analytical Comparison of Air-Cored Coils

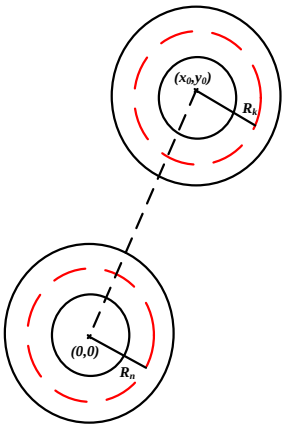

Fig. 3. A coupled circular coil system with primary having $1,2...,n$ turns and the secondary having $1,2...,k$ turns, the radii of the mid current contour of the n^{th} primary turn and k^{th} secondary turn are R_n and R_k.

Consider the case of a circular coil. In such a case, it is possible to evaluate Neumann's integral and calculate the self and mutual inductances. Neglecting transmission line effects and eddy current losses, the mutual inductance M of a coupled circuit can be written as

$$M = \frac{\lambda_{12}}{i_1} = \frac{\mu_0}{4\pi} \oint_{c_1} \oint_{c_2} \frac{d\vec{l}_1 . d\vec{l}_2}{r_{12}} \tag{8}$$

In (8), the two contours c_1 and c_2 represent the contour of current filaments assumed to be in the middle of primary and secondary. However, in case of self-inductance, the same equation can be used with the two contours taken as the mid-current and inner edge contour of the same conductor. Now, consider the case of a misaligned circular coil pair, such a coil pair is indicated in Fig. 3. The inner radius of the primary and secondary are R_i, R_j respectively. In such a case, the partial mutual inductance is written as

$$M_{ij} = \frac{\mu_0}{4\pi} \times \left[\int_{\phi_i=0}^{2\pi} \int_{\phi_j=0}^{2\pi} I d\phi_i d\phi_j \right] \tag{9}$$

Where I is defined as $I =$

$$\frac{R_i R_j \sin\phi_i \sin\phi_j + R_i R_j \cos\phi_i \cos\phi_j}{\sqrt{(R_i \cos\phi_i - (x_0 + R_j \cos\phi_j))^2 + (R_i \sin\phi_i - (y_0 + R_j \sin\phi_j))^2}}$$

The final mutual inductance can be defined for primary having $'n'$ turns and secondary with $'k'$ turns as

$$M = \sum_{i=1}^{n} \sum_{j=1}^{k} L_{ij} \tag{10}$$

The self-inductances can be extracted similarly from (10) by defining the radius of of the middle edge and the inner edge of each turn. Also, in case of an IPT system based on multiple coils, the magnetic and resistive parameters can be evaluated from (7). For other shapes, a detailed evaluation is presented in [7]. For eg: in case of rectangular coils, the mutual inductance can be computed by evaluating

$$M = \frac{\mu_0}{4\pi} \times \begin{bmatrix} \oint_{l_1'} \oint_{l_1} \frac{d\vec{l}_1' . d\vec{l}_1}{r_{1'1}} & \oint_{l_1'} \oint_{l_2} \frac{d\vec{l}_1' . d\vec{l}_2}{r_{1'2}} & \cdots & \oint_{l_1'} \oint_{l_4} \frac{d\vec{l}_1' . d\vec{l}_4}{r_{1'4}} \\ \oint_{l_2'} \oint_{l_1} \frac{d\vec{l}_2' . d\vec{l}_1}{r_{2'1}} & \oint_{l_2'} \oint_{l_2} \frac{d\vec{l}_2' . d\vec{l}_2}{r_{2'2}} & \cdots & \oint_{l_2'} \oint_{l_4} \frac{d\vec{l}_2' . d\vec{l}_4}{r_{2'4}} \\ \oint_{l_3'} \oint_{l_1} \frac{d\vec{l}_3' . d\vec{l}_1}{r_{3'1}} & \oint_{l_3'} \oint_{l_2} \frac{d\vec{l}_3' . d\vec{l}_2}{r_{3'2}} & \cdots & \oint_{l_3'} \oint_{l_4} \frac{d\vec{l}_3' . d\vec{l}_4}{r_{3'4}} \\ \oint_{l_4'} \oint_{l_1} \frac{d\vec{l}_4' . d\vec{l}_1}{r_{4'1}} & \oint_{l_4'} \oint_{l_2} \frac{d\vec{l}_4' . d\vec{l}_2}{r_{4'2}} & \cdots & \oint_{l_4'} \oint_{l_4} \frac{d\vec{l}_4' . d\vec{l}_4}{r_{4'4}} \end{bmatrix} \tag{11}$$

B. Comparison of Coil Shapes and Magnetic Parameters

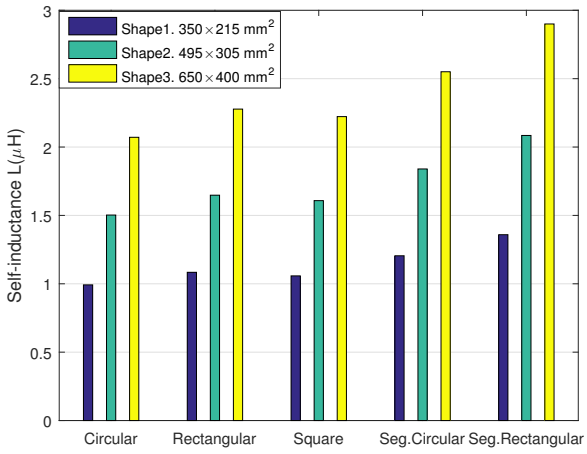

Fig. 4. Analytical computation of self-inductance of various air-cored coils with $N = 1$ and dimensions in Table I. The segmented coils composed of the original shaped coils of half area placed next to each other.

To perform the comparison of coil shape in the performance parameters of IPT systems, we considered the case of charge pad dimensions used in the industry [5], [6]. A number of single-coil based charge pads of variable shapes - circular, rectangular and square are considered as a first step, the parameters are obtained by evaluating (9) and (11). A multi-coil charge pad like segmented circular and rectangular (DD

coil) are then evaluated using (7). To make a comparison, all shapes are analyzed with the same total enclosed area with the individual conductors of 1 mm radius. The segmented coils are also assumed to be lying close to each other without any displacement. The primary and secondary are single turned coils. In case of segmented shapes, the total enclosed area is the sum of individual shapes. Also, similar shapes are compared with both primary and secondary of the same type and the parameters are analyzed. The dimensions of the coils used are tabulated in Table I. The results of self-inductance and coupling comparison are presented in Fig. 4 and Fig. 5. In case of self-inductance, the effect that perimeter has on the same is more predominant than the actual shape in itself. Thus, the segmented shapes have greater self-inductance than non-segmented shapes. In case of mutual inductance, it is the area enclosed by the shapes that matter. It was observed that the circular topology gave the best value of coupling, this can be argued based on the fact that the circular shape has the greatest enclosed area for a given perimeter. Similar results for the circular shape is presented in [8].

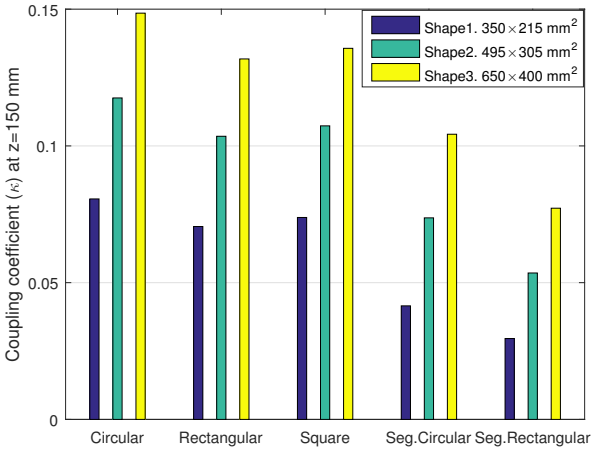

Fig. 5. Analytical computation of coupling of air-cored coils with $N = 1$ and dimensions in Table I. The comparison are for same shapes in both the primary and secondary.

TABLE I
DIMENSIONS OF EQUAL AREA SHAPES CONSIDERED FOR OBTAINING MAGNETIC PARAMETERS

Shape type	Shapes 1.	Shapes 2.	Shapes 3.
Rec. dim.(mm)	350×215	495×305	650×400
Sq. dim.(mm)	274.3×274.3	388.6×388.6	509.9×509.9
Cir. rad.(mm)	154.7	219.2	287.6
Seg. cir. dim.(mm)	109.4	155	203.4
Seg. rec. dim.(mm)	247.4×152	350.0×215.6	459.6×282.8
Area (m^2)	0.0753	0.1510	0.2600

C. Misalignment and Coil Shape Effects

In many applications, the dynamic positioning of the secondary with respect to the primary becomes important. It is important to consider the 3D misalignment for the shapes.

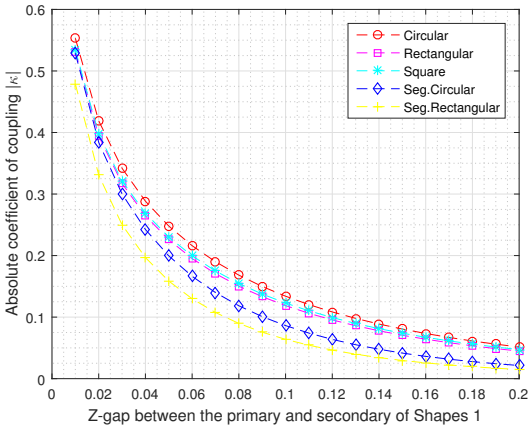

Fig. 6. Absolute coupling as a function of z-gap of *Shapes* 1 from Table I. The z-gaps are variable from 1 cm to 20 cm for perfect lateral alignment.

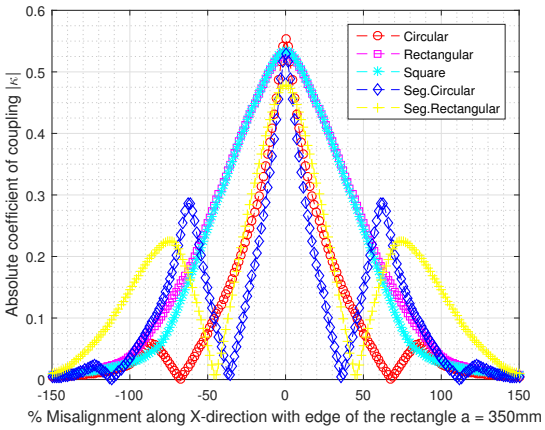

Fig. 7. Absolute coupling as a function of misalignment of Shapes 1 from Table I, when subjected to lateral misalignment. The well aligned position is marked as origin for all shapes at z-gap = 1 cm.

With increasing z-gaps, the coupling tends to decay exponentially for all shapes, this is shown in Fig. 6. For lateral misalignments, the simulations were performed at a z-gap of 1 cm to make effective comparisons. The lateral misalignment characteristic becomes shape dependent as shown in Fig. 7. Similar results for these were obtained, keeping perimeter conserved for all shapes (variable areas) as for multi-turn coils (keeping both area conserved and then perimeter). Hence, it is possible to generalize important observations without loosing scientific credence. Between the circular shape and rectangular/square shape, the major difference is in the misalignment tolerance during lateral misalignment. While the circular shape sees a very sharp drop in the coupling with misalignment, the four sided shapes tend to drop gradually. However, at the best aligned point, circular shape has the highest coupling and is the best solution to IPT systems which are universally well-aligned. This feature is also present in the segmented coils. In addition, it is interesting to note that there exists null-coupling points in the segmented coil misalignment analysis at positions

where a pickup coil completely leaves the zone of its primary. The peak coupling of segmented circular geometry is higher than that of the segmented rectangular geometry. However, the misalignment profile for segmented rectangular coils (DD coils) is greater than that of circular segmented coils and hence it is well suited to EV applications with larger misalignment conditions.

D. Magnetic Power Losses

Quantifying the magnetic losses in an IPT system is important to make a choice for a low loss system, also for optimizing its magnetics. The use of *litz* wire windings is to alleviate high frequency losses in windings. The eddy current losses (skin and proximity effects) can be calculated for a $'n'$ strand of diameter d_i *litz* wire of length l by using [9], [10]:

$$P_s = n \times R_{dc} \times F_s(f) \times \left(\frac{\hat{i}}{n}\right)^2 \times l \tag{12}$$

$$P_p = n \times R_{dc} \times F_p(f) \times \left[H_e^2 + \left(\frac{\hat{i}}{\sqrt{2}\pi d_i}\right)^2\right] \times l \tag{13}$$

In the above equation, the dc strand resistance can be calculated as $R_{dc} = \frac{4}{\sigma \pi d_i^2}$. Also, the external proximity field H_e needs to be calculated analytically by considering the influence of fields due to current in all other strands and turns, on each strand. This can also be accurately computed using FEM analysis. The skin and proximity effect factors can be computed in terms of a simplifying variable $q = \frac{d_i}{\sqrt{2}\delta} = \frac{\sqrt{\omega\mu\sigma}d_i}{2}$ as

$$F_s(f) = \frac{q}{4\sqrt{2}} \left(\frac{ber_0(q)bei_1(q) - ber_0(q)ber_1(q)}{ber_1(q)^2 + bei_1(q)^2} - \frac{bei_0(q)ber_1(q) + bei_0(q)bei_1(q)}{ber_1(q)^2 + bei_1(q)^2}\right)$$

$$F_p(f) = -\frac{q\pi^2 d_i^2}{2\sqrt{2}} \left(\frac{ber_2(q)ber_1(q) + ber_2(q)bei_1(q)}{ber_0(q)^2 + bei_0(q)^2} + \frac{bei_2(q)bei_1(q) + bei_2(q)ber_1(q)}{ber_0(q)^2 + bei_0(q)^2}\right) \tag{14}$$

A detailed model also considering effects of bundles and twisting is proposed in [9]. It is common in many IPT applications to use core to shape the field as well as to enhance coupling and hence power transfered. In such circumstances, the core losses can be evaluated by using the improved Generalized Steinmetz equations (iGSE) [10]. If k, α, β are the Steinmetz parameters and with the understanding of core-loss physics and its dependence on $\frac{dB}{dt}$, the rate of change of core flux density with its temperature T. Then, power-loss per unit volume of the core is given by

$$P_v = \frac{1}{T}\int_0^T k_i \left|\frac{dB}{dt}\right|^\alpha (\Delta B) \mathrm{d}t \tag{15}$$

The Steinmetz coefficient k_i can be calculated from

$$k_i = \frac{k}{(2\pi)^{\alpha-1}\int_0^{2\pi} |\cos\theta|^\alpha |2|^{\beta-\alpha} \mathrm{d}\theta} \tag{16}$$

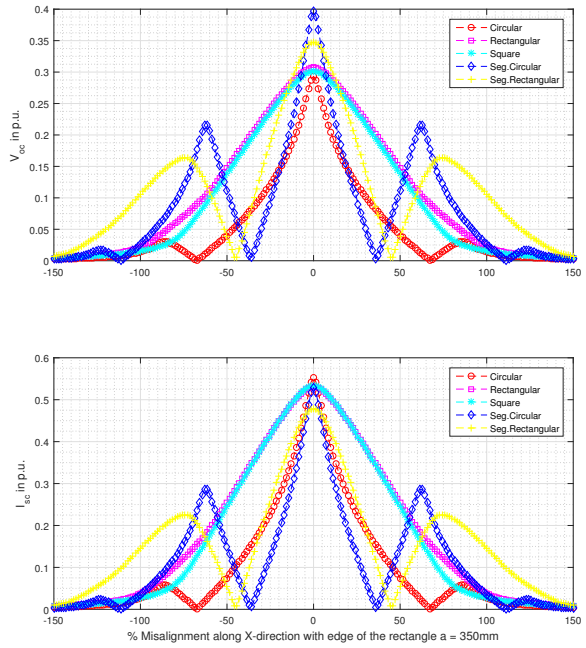

Fig. 8. Open circuit voltage and short circuit current with *Shapes* 1 from Table I for p.u. primary current. The lateral misalignment is simulated at z-gap = 1 cm.

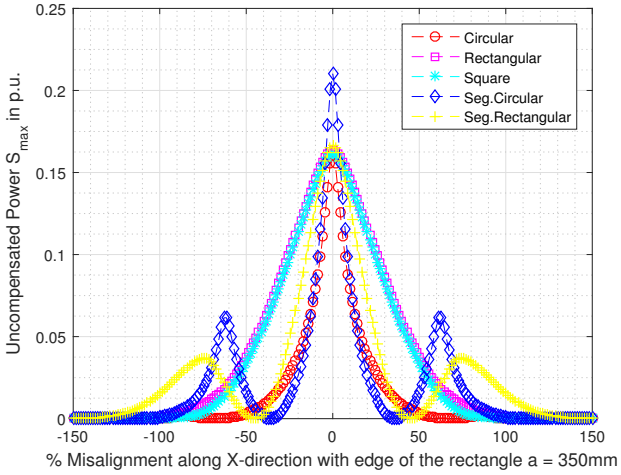

Fig. 9. Uncompensated power of the various shapes with *Shapes* 1 from Table I for p.u. primary current. This characteristic is a product of the two subfigures of Fig. 8.

V. Performance Parameters

The performance parameters that influence the power transferred to the pickup including the open circuited voltage, short circuit current, maximum apparent power and maximum magnetic efficiency V_{oc}, I_{sc}, S_{max}, η_{max}. The load-independent compensation-independent maximum efficiency that can be obtained from a resonant IPT system is given in terms of coupling and native quality factors as [11]

$$\eta_{max} = \frac{k\sqrt{Q_1 Q_2}}{2 + k\sqrt{Q_1 Q_2}} \tag{17}$$

The open-circuit voltage and short-circuit current are defined in (1) and (2). The shape dependent characteristics are analytically calculated and represented in Fig. 8 and Fig. 9. In terms of the absolute power transferred at both the aligned and misaligned points, the performance of segmented coils exceeds that of their non-segmented shapes. The uncompensated power at the minor peaks of the misaligned point is less than 25% of their maxima at best aligned state. This is due to the fact that for both V_{oc} and I_{sc}, the minor peaks are less than 50% of their maximum. The parasitic mutual inductance between the coils of the primary and the secondary also plays a role and has been modeled. Hence, to maintain constant power in segmented coils at minor peaks, transferring power at double currents is a solution. The disadvantage being the copper losses in the charge pad. A control loop can detect the misalignment and decide the current needed to transfer constant power.

It is interesting to also note that the circular shapes in general have a sharper S_{max} peak than the four sided shapes. However, the extension of power profile over larger distances is a requirement for EV applications and hence segmented rectangles perform well. The null-power profile as expected from the coupling variation in Fig. 5 can be eliminated by designing quadrature coils (DDQ chargepad) as in [5].

In the real-world complexities of designing IPT systems for eg: in EVs during motion, dynamic powering, a good choice for the transmitter can be a segmented coil (DD) where the material is optimized for excellent performance than DDQ charge pads inspite of the power null. This being the result of both material saving and the odds of EVs traveling for a large time in the zone of power null. A detailed optimization of such a design is presented in [12]. However, for stationary charging, it would be excellent to research on misalignment tolerant magnetics with a larger zone of power transfer based on DDQ charge pad for both transmitter and receiver. The receiver with DDQ chargepad can then be made inter-operable with the DD transmitter for dynamic powering and this hybrid solution can be good for both modes.

The maximum efficiency contour was calculated from (17). The frequency of operation is taken as $f = 85kHz$. The ac-resistance factor is obtained by considering (14), with litz wire of 600×0.071mm. A tabular implementation for ac-resistance is also available in [13]. The quality factors were determined based on the reactance and the ac resistance at this frequency. The result indicated that segmented circular shape has the highest Q-factor ($Q = 99$). Based on the coupling variation with lateral misalignment, as in Fig. 7, the maximum efficiency contour is plotted in Fig. 10. This contour indicates that it is indeed possible to extend the range of efficiency with segmented (multi-coil) IPT systems.

VI. Performance Limits on Misalignment

It is essentially important to consider the maximum performance contours for the various shapes so as to make a judgment for their operation under conditions of misalignment. Such a limit can be obtained by considering the maximum possible efficiency and maximum possible power transfer at all positions of misalignment. Such a performance contour can establish the magnetic limits of each shape and it becomes possible to compare them. The multi-coil topology (segmented shapes) perform better than the non-segmented shapes, magnetically.

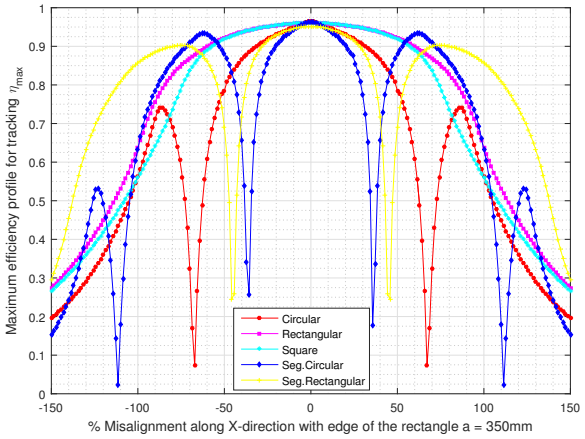

Fig. 10. Maximum efficiency contour with misalignment, here the theoretical limit is plotted for *Shapes* 1 from Table I is simulated at z-gap = 1 cm.

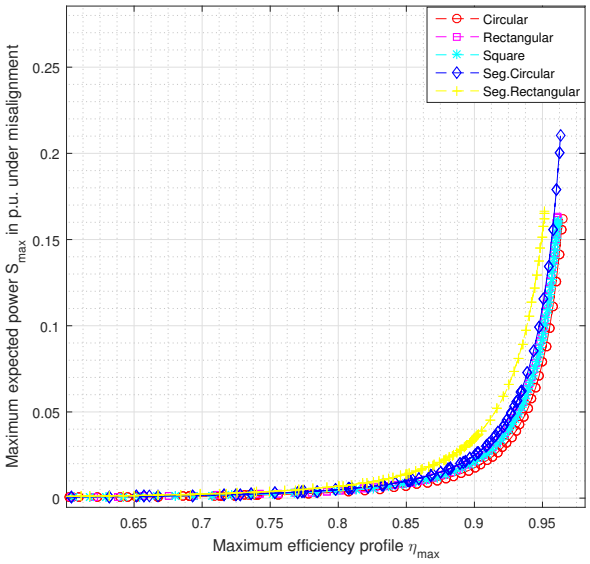

Fig. 11. Theoretical limits of the maximum power on misalignment at p.u. current and max. efficiency at misaligned points with *Shapes* 1 from Table I for p.u. primary current simulated at z-gap = 1 cm.

VII. Conclusion

This paper intends to compare a number of single and multi-coil IPT systems and to compare magnetic parameters holistically. An experimental evaluation of the analytical expressions

for single coil systems has been carried out previously in [7]. Thus, the analysis is accurate.

The main contribution of this paper has been to extend the theory to multi-coil IPT systems based on a matrix method that considers the linearity of the system. For a large air-gap transformer, the system is generally linear even with the presence of a high permeability material like steel, ferrite etc. The only non-linearity can be saturation at very low air-gaps or during faults, which can be controlled by having a feedback control loop that can bring the system back to the linear region or cuts out the fault. Some important results obtained are

1) In case of linear magnetic systems, it is possible to reduce a linear multi-coil primary, multi-coil secondary system to a single coil primary, single coil pickup system.
2) Circular coils have the largest area for a given perimeter and are effective for IPT systems with little misalignment.
3) Rectangular shape has a larger misalignment-band than circular shape and is effective in terms of gradient of coupling than circular shape and hence has an excellent tolerance to misalignment. However, it has lesser coupling at the best aligned point than the circular shape.
4) Segmented shapes can effectively extend the misalignment tolerance of charge pads. Segmented rectangle can extend more effectively than segmented circular.
5) The performance limits of efficiency and maximum power output suggests that segmented rectangle can perform the best among various shapes compared for lateral misalignment.
6) The uncompensated power at the minor peaks of multi-coil IPT system is less than 25% of the best aligned state (maxima). This is because both V_{oc} and I_{sc} are less than 50% each.
7) The choice of shapes and their segmentation influence both the best aligned magnetic parameters as well as misalignment parameters (for pickup with a relative velocity For eg: EVs, MRI machines and traction applications).
8) For numerical studies like FEM, it is possible to superpose the results from simpler single coil systems and build the multi-coil system using (7) and Fig. 2.

ACKNOWLEDGMENT

The first author would like to thank Udai Shipurkar, Nils van der Blij and Aditya Shekhar for interesting discussions that improved the manuscript.

REFERENCES

[1] V. Prasanth and P. Bauer, "Distributed IPT Systems for Dynamic Powering: Misalignment Analysis," *IEEE Transactions on Industrial Electronics*, vol. 61, no. 11, pp. 6013–6021, nov 2014.

[2] G. A. Covic and J. T. Boys, "Inductive power transfer," *Proceedings of the IEEE*, vol. 101, no. 6, pp. 1276–1289, June 2013.

[3] A. Shekhar, M. Bolech, V. Prasanth, and P. Bauer, "Economic considerations for on-road wireless charging systems-A case study," in *Emerging Technologies: Wireless Power (WoW), 2015 IEEE PELS Workshop on*. IEEE, 2015, pp. 1–5.

[4] A. Shekhar, V. Prasanth, P. Bauer, and M. Bolech, "Generic methodology for driving range estimation of electric vehicle with on-road charging," in *Transportation Electrification Conference and Expo (ITEC), 2015 IEEE*. IEEE, 2015, pp. 1–8.

[5] J. T. Boys and G. A. Covic, "IPT Fact Sheet Series : No . 2 Magnetic Circuits for Powering Electric Vehicles," Tech. Rep. 2, 2014.

[6] ——, "Inductive power transfer systems (IPT) Fact Sheet: No . 1 Basic Concepts," Tech. Rep. 1, 2013.

[7] V. Prasanth, P. Bauer, and J. A. Ferreira, "A sectional matrix method for IPT coil shape optimization," in *Power Electronics and ECCE Asia (ICPE-ECCE Asia), 2015 9th International Conference on*. IEEE, 2015, pp. 1684–1691.

[8] R. Bosshard, J. Muhlethaler, J. W. Kolar, and I. Stevanovic, "Optimized magnetic design for inductive power transfer coils," in *2013 Twenty-Eighth Annual IEEE Applied Power Electronics Conference and Exposition (APEC)*. IEEE, mar 2013, pp. 1812–1819. [Online]. Available: http://ieeexplore.ieee.org/lpdocs/epic03/wrapper.htm?arnumber=6520541

[9] C. R. Sullivan and L. W. Losses, "Analytical model for effects of twisting on litz-wire losses," in *Control and Modeling for Power Electronics (COMPEL), 2014 IEEE 15th Workshop on*, June 2014, pp. 1–10.

[10] J. Muhlethaler, J. W. Kolar, and A. Ecklebe, "Loss modeling of inductive components employed in power electronic systems," in *8th International Conference on Power Electronics - ECCE Asia*. IEEE, may 2011, pp. 945–952. [Online]. Available: http://ieeexplore.ieee.org/lpdocs/epic03/wrapper.htm?arnumber=5944652

[11] H. Takanashi, Y. Sato, Y. Kaneko, S. Abe, and T. Yasuda, "A large air gap 3 kw wireless power transfer system for electric vehicles," in *Energy Conversion Congress and Exposition (ECCE), 2012 IEEE*, Sept 2012, pp. 269–274.

[12] S. Bandyopadhyay, V. Prasanth, P. Bauer, and J. Ferreira, "Multi-Objective Optimisation of Distributed IPT Systems for charging of Electric vehicles," in *IEEE Transportation Electrification Conference and Expo, 2016 IEEE*, 2016.

[13] F. E. Terman *et al.*, "Radio Engineer's Handbook," 1943.